Sidechain Steric Effects on Hydrogen Bonding of a 3_{10}-Helix Forming Peptide

Mike Thorgersen

Faculty Sponsor: Adrienne Loh, Department of Chemistry

ABSTRACT

The hydrogen bonding strengths in a 3_{10}-helix forming peptide were analyzed in order to gain an understanding of the effects of steric hindrance on peptide flexibility. The peptide studied was composed of eight amino acids, the fourth and fifth of which were alanine, and the rest of which were α-aminoisobutyric acid (Aib), a sterically hindered α,α-dialkylated amino acid that forces the peptide into a 3_{10}-helical conformation. Alanine is less sterically hindered than Aib, allowing for greater flexibility in the center of the peptide. ^{1}H NMR spectra were obtained of samples of the peptide dissolved in CD_3OD. The decay of the amide ^{1}H NMR signals over time due to the exchange of the amide protons with methanol deuterons was analyzed using pseudo first order kinetics at several temperatures. The relative strength of each hydrogen bond was characterized in terms of the activation barrier to exchange using the Arrhenius equation. The data shows that one face of the center of the helix is less rigid than the other, having amide protons with lower activation barriers to exchange and higher exchange rate constants. These more accessible amide protons are on the opposite face of the helix from the two alanine residues, and the hydrogen bond that spans both alanine residues is broken in CD_3OD. This indicates that the decreased steric hindrance in the center of the helix has a destabilizing effect on the structure of the peptide.

INTRODUCTION

Proteins are macromolecules found in living systems that are composed of amino acids connected with peptide bonds. There are four levels of protein structure. The primary structure of a protein is the sequential order in which different amino acids are linked together. The secondary structure of a protein is how this primary structure folds together to form various structures such as helices and pleated sheets. The tertiary structure of a protein involves how these secondary structures interact with each other forming a protein. If several proteins come together they have quaternary structure (1). The structure of a protein has been shown to have a profound affect on the function of the protein. For example, the change of even one amino acid in the structure of enzymes (proteins that catalyze reactions) has been known to disable the enzyme so that it cannot catalyze the reaction (1).

In this research, the effects of amino acid side chain sterics on a protein secondary structure known as the 3_{10}-helix are being studied. The 3_{10}-helix is characterized by having an i→i+3 hydrogen bonding pattern (2). This means that the amide proton of one amino acid residue is hydrogen-bonded to the carbonyl group on the amino acid three residues away. The 3_{10}-helix is not as common a secondary structure as the α-helix, but it does account for

approximately 10% of the helical structures found in proteins studied by x-ray crystallography (3). There is also evidence that the 3_{10}-helix may be involved as an intermediate in α-helix formation (4,5).

Peptides composed entirely of the amino acid Aib (Fig. 1) have been shown to form 3_{10}-helices (6). It is believed that Aib-containing peptides form this helical structure because of the high steric hindrance experienced by the two α-methyl groups in the residue (7). In fact, the effects of steric hindrance in Aib are so significant that structures of Aib-rich 3_{10}-helical peptides have been found to be stable at temperatures as high as 120 °C (8), and substitution of only one alanine for Aib in a 61 residue protein fragment significantly improved the thermal stability of the protein (9). However, studies have also shown that Aib-rich peptides that contain two consecutive non-Aib residues have deviations in structure from the ideal 3_{10}-helix (2, 10, 11).

The peptide tBoc-$B_3A_2B_3$-NHMe (AA45, Fig.1) was designed to study the effects of steric hindrance on the formation of 3_{10}-helices in Aib peptides. In this peptide, the forth and fifth residues of the peptide are the less sterically hindered amino acid alanine (Ala, A). Previous research on this peptide has shown that it is 3_{10}-helical, and that high concentrations of hydrogen-bonding solvents like DMSO cause the hydrogen bond to the amide of Aib6 to break (2). It is believed that this breakage occurs because of the lowered steric hindrance in the center of the structure. In this research, the strengths of the hydrogen bonds in AA45 were studied in methanol in order to obtain more information on the effects of steric hindrance on the flexibility and dynamics of Aib-containing helices.

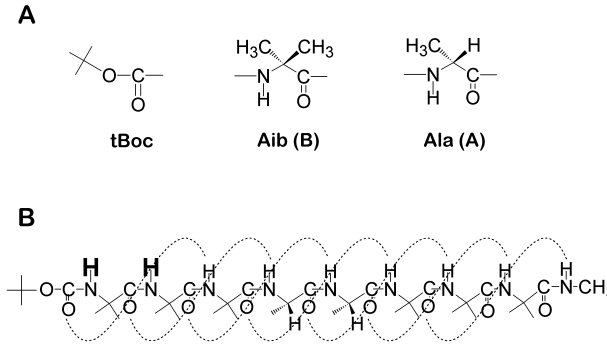

Figure 1: A The building blocks of tBoc-$B_3A_2B_3$-NHMe (AA45). Aib (α-aminoisobutyric acid) differs from the common amino acids in that it is dialkylated at the α-carbon. B The 3_{10}-helical hydrogen bonding pattern in AA45. The two N terminal α-hydrogens (in bold) are not intramolecularly hydrogen bonded.

METHODS

Chemical shift determination:

The amide proton peak assignments were previously determined in 100% DMSO-d6 (2). They were mapped into methanol by taking NMR spectra of solutions prepared by adding aliquots of CD_3OH to a 2 mM solution of tBoc-$B_3A_2B_3$-NHMe (AA45) dissolved in DMSO-d6 until a 50% DMSO/CD_3OH solvent ratio was reached. Next aliquots of DMSO-d6 were added to a 2 mM solution of AA45 dissolved in CD_3OH until a 50% DMSO/CD_3OH solvent ratio was reached. All spectra were obtained on a Bruker AC 300 MHz spectrometer at 305 K using solvent presaturation on the alcohol proton of CD_3OH. A pulse angle of 90° was used,

and a total of 32 scans were obtained for each spectrum. Chemical shifts were referenced to TMS at 0 ppm.

Exchange experiments:

1_H NMR spectra were obtained of a solution of 2 mM AA45 in CD_3OD at 303, 309, 315, 321, and 328 K as a function of time. The spectrometer was pre-shimmed on CD_3OD, and time was started when the CD_3OD was added to the dry AA45 sample. All spectra were obtained using a pulse angle of 52° and 32 scans. Using the program WinNuts (Acorn NMR), the intensity of each proton peak at each time interval was integrated relative to the peak from the tBoc and methyl protons, which do not exchange with deuterons from the solvent. Due to overlap in chemical shift, amide protons 3 and 5 were integrated together as were amide protons 7 and 8. Baselines were corrected using a polynomial fit.

Kinetics:

The reaction equation for the exchange of peptide amide protons with deuterons from the solvent is:

$$NH + CD_3OD \rightarrow CD_3OH + ND \quad (1)$$

Since the reaction was performed in a large excess of CD_3OD, the concentration of CD_3OD did not change significantly during the reaction. Therefore the data was analyzed using pseudo first order kinetics. Under these conditions, the rate law for reaction (1) is given by:

$$Rate = k'[NH] \quad (2)$$

where the pseudo first order rate constant, k', is given by:

$$k' = k[CD_3OD] \quad (3)$$

Values of the pseudo first order rate constant for each amide were obtained from a linear least squares analyses of the relative integrated areas (I) of the amide proton peaks as a function of time (equation 4).

$$\ln I = \ln I_0 - k't \quad (4)$$

where I_0 is the relative integrated area at t=0. The activation energy of each peak was calculated using a linearized version of the Arrhenius equation (equation 5).

$$\ln k' = \ln A - \frac{E_a}{RT} \quad (5)$$

where A is the collision frequency, E_a is the activation energy, R is the ideal gas constant, and T is the temperature in K. Estimates of the collision frequency contained too much error to be reported reliably. All other errors are reported as standard deviations.

RESULTS

The chemical shifts of the amide proton peaks varied with solvent composition as the peptide was dissolved in various combinations of DMSO and CD_3OH (Fig. 2). A plot of the chemical shift of the amide protons versus % CD_3OH added revealed two different amide proton trends. The chemical shifts of the amide protons of Aib1, Aib2, and Aib6 (black symbols) shifted upfield upon the addition of CD_3OH, where those of the other amide protons (gray symbols) shifted downfield. Aib1 and Aib2 are located at the N-terminus of the peptide, and thus their amide protons are not intramolecularly hydrogen bonded (Figure 1). According to the 3_{10}-helical hydrogen bonding pattern, the amide proton of Aib6 should be hydrogen bonded to the carbonyl of Aib3 resulting in a hydrogen bond that would span the two alanine residues (4 and 5). However, the similar response of the Aib6 amide proton to the change of solvent to those of Aib1 and Aib2 suggests that the amide proton of Aib6 is also not hydrogen bonded. This hydrogen bond has been previously shown to be broken in DMSO (a hydrogen-bonding solvent) but not in $CDCl_3$ (a non-hydrogen-bonding solvent) (2). The apparent broken hydrogen bond to Aib6 is consistent with these previous reports since CD_3OH is also a hydrogen-bonding solvent.

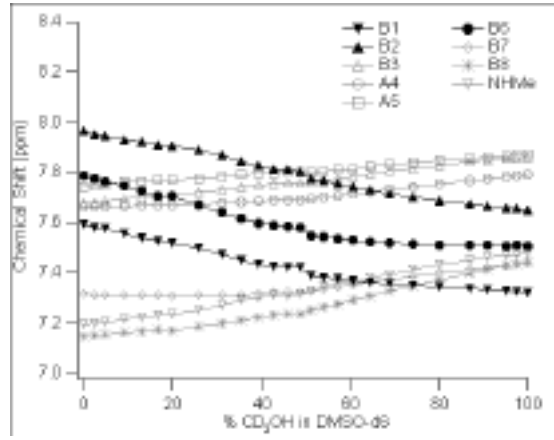

Figure 2: Mapping of the amide proton chemical shifts in AA45 from DMSO-d6 to CD3OH. The protonated version of methanol (CD3OH rather than CD3OD) was used to avoid a decay in the amide proton signal due to exchange with the solvent.

Sample NMR spectra of the amide region of AA45 as a function of time are shown in Figure 3. The exposure of the peptide to the solvent cause the amide protons to exchange with the acidic deuteron on CD_3OD, resulting in a decay in the integrated area over time. It can be seen that some of the amide protons decay at a faster rate than others. For example the

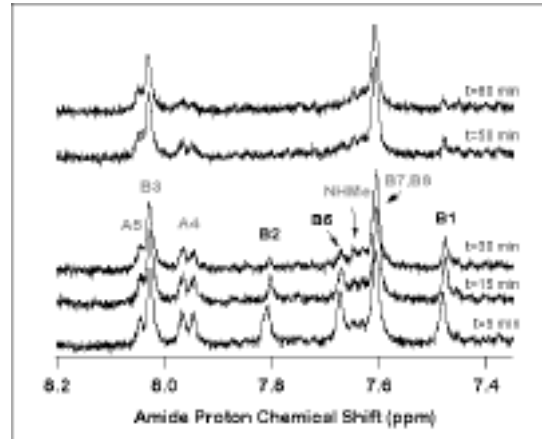

Figure 3: The amide region of a few representative ^{1}H NMR spectra of AA45 in CD_3OD over time. The black lettering indicates amide protons that are not hydrogen-bonded (Aib1, Aib2, Aib6); all others are shown in gray.

amide protons of Aib1 and Aib2 are completely exchanged by 50 minutes, while those of Aib7 and Aib8 still have high intensities at 80 minutes. Due to overlap between the chemical shifts, amide protons 3 and 5 were integrated together as were amide protons 7 and 8.

The rate constants for the exchange of amide protons for deuterons at various temperatures are shown in Figure 4. As was seen in the raw spectra, different regions of the peptide exchange with different rate constants. The two amide protons at the N-terminus of the peptide (Aib1, Aib2) had large rate constants, indicating exposure to the solvent. Neither of these amide protons is hydrogen bonded to a carbonyl group. The amide protons of Aib7, Aib8, and NHMe (amide 9) all had relatively small rate constants indicating that they are not as exposed to the solvent. These amide protons are located at the C-terminus of the peptide. In the center of the peptide, the amide protons of Aib6 and Ala4 had larger rate constants than those of Aib3 and Ala5.

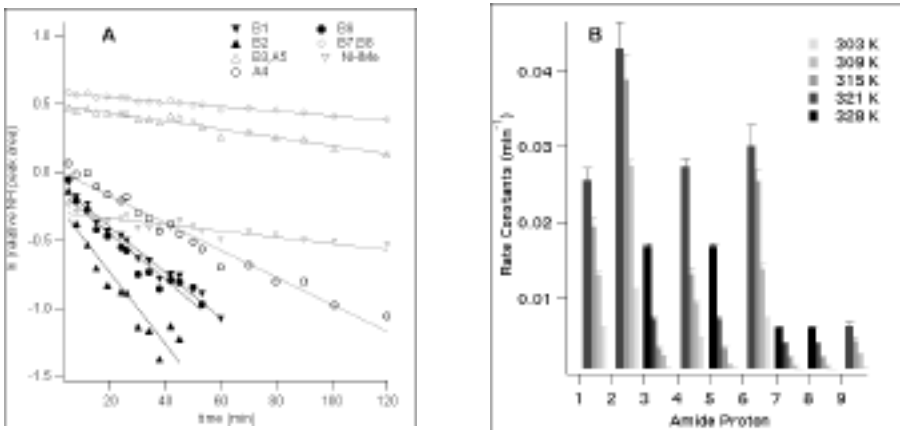

Figure 4: Rate constants for exchange of the amide protons in AA45 with CD_3OD at various temperatures. A: Pseudo-first order plots at T= 305 K. B: Pseudo-first order rate constants.

As expected, as the temperature of the exchange reaction was increased, the pseudo-rate constants for exchange increased. Not all amide protons had observable rate constants at all temperatures. For example, at 328 K all amides except Aib3, Ala5, Aib7, and Aib8 exchanged too quickly to measure. This suggests that these amide protons are not as open to exchange as those amide protons that have faster rate constants. At lower temperatures such as 303 K, the slower exchanging amide protons did not exchange enough to obtain reliable rate constants.

The activation barriers to exchange were calculated from a linear fit of the pseudo rate constants to equation 5 (Figure 5). The first two amide protons are not intramolecularly hydrogen bonded, and had low activation barriers to exchange. At the C-terminus of the peptide, the last three amide protons had high activation barriers. Following the same trend observed in the rate constants at a given temperature, the amide protons of Ala4 and Aib6 had lower activation energies than those of Aib3 and Ala5, which had the highest activation exchange barriers to exchange in the peptide. Interestingly, the amide protons of Ala4 and Aib6 are located on the same face of the helix (Figure 6), while those of Aib3 and Ala5 are on the opposite face of the helix.

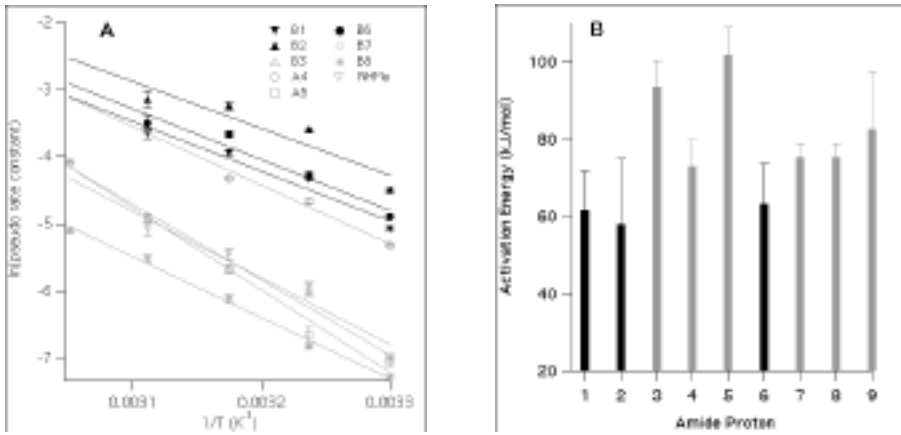

Figure 5: Comparison of the activation energies for the amide protons in AA45. The unusually low activation energies for amide protons 4 and 6 relative to the other central amides indicates increased accessibility in the center of the helix.

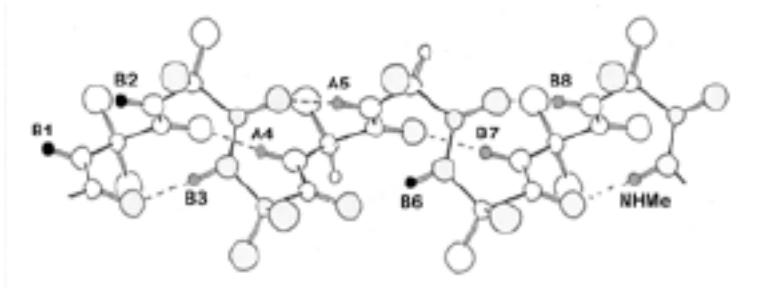

Figure 6: The three-dimensional ball and stick diagram shows the 3_{10}-helical structure of AA45. The amides of Ala4 and Aib6 are on the back face of the helix, on the same side as the sidechains of the two Ala residues. The amides of Aib5 and Ala4 are on the front face of the helix.

DISCUSSION

The 3_{10}-helical peptide tBoc-$B_3A_2B_3$-NHMe (AA45) was synthesized and studied in order to understand the effect of sterics on the structure and flexibility of 3_{10}-helical Aib peptides. This peptide is composed mostly of the sterically hindered amino acid Aib. However the forth and fifth amino acids out of eight are the less sterically hindered amino acid Alanine. An eight residue peptide composed entirely of Aib (B8) has previously shown flexibility only near the N-terminus of the peptide where the amide protons were not intramolecularly hydrogen bonded, and increasing stability along the chain towards the C-terminus (2, 12). This study on AA45 reveals a different behavior, indicating that the lowered steric hindrance in the center of the peptide affects the overall structure and flexibility of the peptide.

Mapping experiment:

In the mapping experiment, two trends of behavior were noted for the amide protons of AA45. The response of the amide protons to a change in their environment can indicate the

relative amount of solvent accessibility the amide protons experience. Most of the amide protons shifted downfield as CD_3OH was added to their DMSO environment. However, amide protons 1, 2, and 6 shifted upfield as CD_3OH was added. The difference in the behavior for amide protons 1 and 2 can be explained in that these amide protons are at the N-terminal end of the peptide and thus are not intramolecularly hydrogen bonded. They are therefore more exposed to the solvent than the other amide protons. In contrast, amide proton 6 is located so that it would be hydrogen bonded to the carbonyl of Aib3; this hydrogen-bond would span the two alanine residues. The fact that the chemical shift of this amide proton changed in the same way as amide protons without intramolecular hydrogen bonds indicates that the hydrogen bond to the sixth amide proton is broken in the solvents used for the mapping experiment. This observation is supported by previously obtained temperature perturbation studies on AA45 in DMSO-d6, in which amide protons 1, 2, and 6 were shown to have a response to a change in temperature that is characteristic of non-hydrogen bonded amides (2). Thus, the lowered steric hindrance of the alanine residues affects the flexibility of the helix in the region of amide proton 6 to the extent that the hydrogen-bond spanning the two alanine residue is broken. However, two-dimensional NMR studies on AA45 in DMSO-d6 show that the overall helical structure remains intact despite the broken hydrogen bond to Aib6 (2).

Rate Constant Data:

The values of the pseudo-rate constants for the exchange of the amide protons with deuterons from the solvent indicates the degree of exposure of each amide proton to the solvent. In B8, the pseudo-rate constants for all amides decreased along the chain towards the C-terminus, with the exception of the two N-terminal and the last C-terminal amide proton (11). This trend is not noted in AA45. The lowered steric hindrance in the center of the peptide causes the behavior of the amide proton exchanges to change. In this peptide, amide protons 4 and 6 had unusually high pseudo-exchange rate constants. Based on the results from the mapping experiment, the exchange rate for amide proton 6 was expected to be higher because of the broken hydrogen bond. However, the elevation of the pseudo-rate constant for Ala4 indicated that the lower steric hindrance in the center of the peptide was in some way destabilizing a center portion of the helix. In contrast, the amides of Aib3 and Ala5 did not show this increase in exchange rate, suggesting that the destabilization effect is localized to one face of the helix.

Activation Barrier Data:

The activation barrier to the exchange of an amide proton provides an indication of the flexibility of the peptide in the region where the amide proton is located. In studying AA45, low activation barriers were found near the N-terminus, indicating flexibility in this region. In contrast, the C-terminal amides had high activation barriers indicating a more rigid region of the helix. In the center of the helix, the activation barriers for amide protons 4 and 6 were lower than those of amide protons 3 and 5. These differences are presumably caused by the lowered steric hindrance of the center of the peptide since this effect was not noted for the homo-Aib peptide B8 (11). Amide protons 4 and 6 are on the same face of the 3_{10}-helix. One possibility that has been previously suggested (2) is that the lowered steric hindrance allows the helix to pinch at the two Ala sidechains, causing the hydrogen bond to the amide proton of Aib6 to break. As a result, the entire face of the helix containing amide proton 6 would be opened up to the solvent and exposed to exchange, while the opposite face containing amide

protons 3 and 5 would be constricted and thus more protected from exchange. Unfortunately, the degree of error in the Arrhenius plots prohibits a definitive statement in this regard. This is due in part to the small range of temperatures studied. Error was also introduced into the Arrhenius plots due to temperature regulation errors in the NMR instrument. In order to decrease the amount of error several more exchange experiments should be performed at different well regulated temperatures.

It is also curious that in the solvent composition mapping experiment (Figure 2), amide proton 4 acted like the main group of amide protons (Aib3, Ala5, Aib7, Aib8, NHMe9), whereas in the exchange experiments (Figure 4, 5) amide proton 4 acted in a manner similar to that of Aib6. Clearly more information is needed on the role of Ala4 in the stability and flexibility of the AA45 helix.

In conclusion, it was discovered in the study of AA45 that steric hindrance had a significant effect on the structure of the 3_{10}-helix. The lowered steric hindrance in the center of the peptide caused the breakage of a hydrogen bond, and also appeared to cause the helix to bend in the center. These types of effects add to the collective understanding of the forces that govern protein stability and structure, and thus to the connection between protein structure and function.

REFERENCES

1. Creighton, T.E., *Proteins: Structure and Molecular Properties*. 2nd ed. (1993) NY: WH Freeman & Co.
2. Pettijohn, A. (1995) *Ph.D. Thesis*, Ithaca, Cornell University.
3. Barlow, D.J. and Thornton, J.M. (1998) Helix geometry in proteins, *J. Mol. Biol. 201*, 601-619.
4. Sundaralingham, M. and Sekharudu, Y. C. (1989) Water-inserted α-helical segments implicate reverse turns as folding intermediates, *Science*, *244*, 1333-1337.
5. Tirado-Rives, J. and Jorgensen, W. L. (1991) Molecular dynamics simulations of the unfolding of an α-helical analogue of ribonuclease A S-peptide in water, *Biochemistry*, *30*, 3864-3871.
6. Toniolo, C., et al. (1985) Conformation of pleinomers of Aib, *Macromolecules 18*, 895-902.
7. Paterson, Y., Rumsey, S.M., Benedetti, E., Nemethy, G., and Scheraga, H.A. (1981) Sensitivity of polypeptide conformation to geometry theoretical conformational analysis of oligomers of α-aminoisobutyric acid, *J. Amer. Chem. Soc. 103*, 2947-2955.
8. Augspurger, J.D., Bindra, V.A., Scheraga, H.A., and Kuki, A. (1995) Helical stability of de novo designed α-aminoisobutyric acid-rich peptides at high temperatures, *Biochemistry, 34*, 2566-2576.
9. De Fillippis, V., De Antoni, F., Frigo, M., Polverino de Laureto, P., and Fontana, A. (1998) Enhanced protein thermostability by Ala→Aib replacement, *Biochemistry, 37*, 1686-1696.
10. Basu G., and Kuki A. (1992) Conformational preferences of oligopeptides rich in α-aminoisobutyric acid. II. A model for the 3_{10}/α-helix transition with composition and sequence sensitivity, *Biopolymers. 32*, 61-71.
11. Balaram, H., Sukumar, M., and Balaram, P. (1986) Stereochemistry of α-aminoisobutyric acid peptides in solution: conformations of decapeptides with a central triplet of contiguous L-amino acids, *Biopolymers, 25*, 2209-2223.

12. Rivard, T. and Loh, A. P., (1999) Determination of Amide Proton Solvent Accessibility from Kinetic Studies of H-D Exchange, *10th Annual Argonne Symposium for Undergraduate Research in Science, Engineering and Mathematics*, Chicago, IL.

ACKNOWLEDGEMENTS

This work was made possible through the generous support of the University of Wisconsin-La Crosse Faculty Research Grant Program. Travel to present this research at the Annual Meeting of the Biophysical Society was made possible by a College of Science and Allied Health Travel Grant award to M. Thorgersen. The authors would also like to thank previous researchers Matthew Geisler, Todd Rivard, Rachael Hoffman, Brian Trewyn and Joe Davis, and current researcher Larry Masterson for all of their contributions to the Aib projects. Finally, M. Thorgersen would like to thank Dr. Loh for all her instruction and time as a research mentor.